Effect of Air Gaps on Photovoltaic Operating Temperature and Heat Gain Penetration into Buildings

Piyatida Trinuruk and Chumnong Sorapipatana
The Joint Graduate School of Energy and Environment (JGSEE),
King Mongkut's University of Technology Thonburi, Bangkok 10140, Thailand and
Center for Energy Technology and Environment, Ministry of Education, Thailand.

Abstract

An installed photovoltaic (PV) module on a building envelope is beneficial not only for generating PV clean electricity, but also for reducing the cooling load of a building, provided that its installation is properly designed. Spacing of an air gap between the PV module and the exterior surface of the building envelope plays an important role in the PV modules' performance and the heat gain penetration into the building, because it directly affects heat transfer from the PV module to the building envelope. PV module installations over a building envelope can be useful, especially in Thailand, where the climate is hot and humid, if it helps to minimize the heat gain penetration into the building, and at the same time, can also generate clean electricity from the PV modules.

In this study, a simulation model based on one-dimensional transient heat transfer has been developed to investigate a proper air gap for a PV module installation, for fixing on a vertical wall facing southward. The accuracy of the developed model was verified with an outdoor experiment by a test rig under clear sky conditions in Bangkok, Thailand. The model's validation showed a satisfactory result of predicted temperatures. The simulation results showed that an increase in the air gap's spacing can improve the performance of the PV module, at the same time, it can also reduce the heat gain penetrating into the building. Although a PV module can be used as a shading device to reduce heat gain for a building envelope, it can also generate a large amount of heat gain penetration into the building envelope. This is a consequence of high thermal absorbtivity of the PV module, which results in intensively absorbing large amounts of heat within its body as it receives shortwave solar radiation from the sum and re-radiates it back to the building's surface. Thus, a proper air gap space design is quite important for the installation.

It was also found that the change of amounts of heat gain penetration into a building is much more sensitive than the change of electricity generation of the PV module performance, due to variations of the air gap. Thus, the judgment of a proper air gap spacing design should be given first priority on the reduction of the heat gain into the building. A minimum air gap of 50 mm is recommended for a single PV module, in vertical facing southward installations, for tropical climates.

Keywords: Photovoltaic module, Spacing, Ventilated air, Heat gain, Electricity generation, One-dimensional transient heat transfer

1. Introduction

An installation of photovoltaic (PV) modules over a building wall generally has advantages over a conventional building wall in such a way that its installation can serve multi-purpose functions, i.e., it can cover a wall from exposure to solar irradiance as a shading device and it can also generate clean electricity simultaneously. Superficially, it seems that the installation of the PV module over a wall would help to protect heat gains penetrating into the building. Consequently, cooling loads of air conditioning systems of the building can be reduced, which in turn would reduce the electrical energy consumption in the building, especially in tropical regions like Thailand, where approximately 75% of the total electricity in a household sector is consumed by air conditioning systems [1].

Unfortunately, the installation of a PV wall does not always reduce the heat gain penetration into the building as expected, if the gap between the back surface of a PV module and the exterior surface of the building wall is not properly designed. It can transfer more heat gain and penetrate into the building, due to high thermal radiation from the back surface of the PV module, and poor heat cooling by the air inside the gap. It also affects the high operating temperatures of PV cells inside the module. This effect eventually decreases the efficiency of a PV module's electricity generation performance. In general, with a rise of 1^{o}C of a PV module temperature from the standard reference temperature of the PV module at 25^{o}C, its performance will decrease by 0.37%-0.52% for crystalline silicon cells and 0.1-0.45% for thin film silicon cells, respectively [2].

In most practices for PV module installation over a building envelope, an air gap is generally provided at the back of the installed PV module. The purpose of the air gap is for cooling the PV module. Several research groups have investigated the impacts of the air gap on ventilation capacity of the PV module, and the building space's heating and cooling loads and their effect on the PV module's performance. They found that the cooling effect of the air gap to cool the PV module was subject to the air gap's configuration and the flow's characteristic of the air inside the gap. By comparing between ventilated and non-ventilated air gaps, it was found that a well designed, ventilated air gap can lower the operating temperature of the PV module by at least 15-26^{o}C as compared to the non-ventilated one [3-4]. The active ventilation by a force convection process is also significantly cooling down the PV module's temperature more than that of natural convection [5]. Additionally, the ventilated air gap for the PV module installation not only lowers the PV module operating temperature, but it also has an effect on reducing the peak temperature of the exterior surface of a building envelope due to the shading effect of the PV module. Thus, the building cooling loads can be decreased [3-4, 6].

However, all research work mentioned above is only concerned with the effects of ventilation configurations such as total encapsulation of air gaps, total opening of air gaps, two opening ends of air gaps, etc. So far there has not been any attempt to study the effect of the air gap's spacing on the PV module's performance and the heat gain penetration into the building. Hence, appropriate spacing of the air gap for the PV module installation should be evaluated for good practice of PV module installation over a building's walls, especially for those installations in tropical climates, where only a few studies have been conducted.

The aims of this study are:

(1) to investigate the effect of air gap spacing to the PV module's operating temperature, the annual amount of electricity generation and the annual amount of the heat gain penetration into a building,

by using one-dimensional transient heat transfer modeling, which verifies the accuracy of the model with the experiment.

(2) to compare the heat gain penetration into a building between two building facades, one is installed with PV module and the another one is without any installed PV module.

The scope of this study is limited only to the orientation of the PV module facing due southward under the assumption of clear sky conditions. In this case, a PV module received the maximum amount of solar irradiance over an entire year.

2. Mathematical Modeling Formulation of the Energy Balance of an Installed PV Module

In this Section, theoretical modeling of an installed PV module on a building wall is given for predicting the amount of electricity generation from a PV module and the heat gain penetrating into a building. Fig.1 illustrates the heat transfer processes occurring on a PV module mounted on a wall with fully opening air gap to the ambient, around all edges of a PV module.

2.1 Energy Balance of a PV Module

Since only a partial amount of solar irradiance falling on a PV module can be absorbed and converted to electricity by solar cells, the rest of it is lost as heat by means of heat transfer. A balance of energy of the PV module can be given by the equation as shown below:

$$\dot{I}_t(\alpha\tau)_{pv} = q''_{c,f} + q''_{r,f} + q''_{c,a1} + q''_{r,a} + E''_{pv} + q''_{st,pv} \quad (1)$$

where $\dot{I}_t$ is the solar irradiance incident on tilted surface (W/m^2), $(\alpha\tau)_{pv}$ is the absorptivity-transmittivity of the PV module, $q''_{c,f}$ and $q''_{r,f}$ are the rate of heat convection and the rate of radiative heat exchanged at the front PV surface of the module (W/m^2), respectively. $q''_{c,a1}$ and $q''_{r,a}$ are the rate of heat convection due to the mass of air in the gap and the rate of radiative heat exchanged at the back PV module's surface (W/m^2), respectively. E''_{pv} is the electricity generated from the PV module (W/m^2) and $q''_{st,pv}$ is the accumulated heat rate within the PV module (W/m^2).

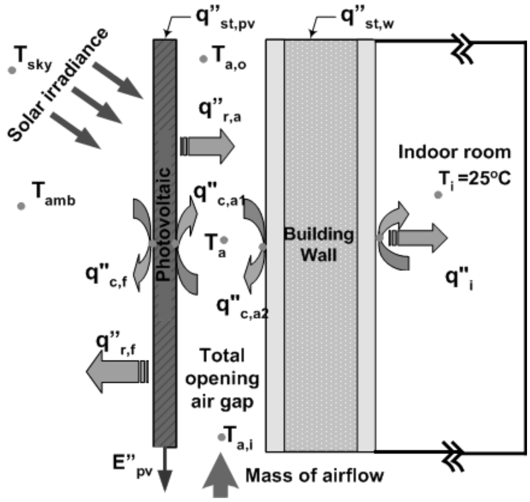

Fig. 1 The heat transfer processes of a PV module mounted on a building wall

Each parameter in Eq.(1) can be rewritten in terms of different temperatures as follow:

$$q''_{c,f} = h_{c,f}(T_{pv} - T_{amb}), \quad (2)$$

$$q''_{r.f} = h_{r,f}(T_{pv} - T_{sky}), \quad (3)$$

$$q''_{c,a1} = h_{c,a1}(T_{pv} - T_a), \quad (4)$$

$$q''_{r,a} = h_{r,a}(T_{pv} - T_{wo}), \quad (5)$$

where $h_{c,f}$ and $h_{r,f}$ represent the coefficient of heat convection and thermal radiation at the front PV module's surface (W/Km^2), respectively. $h_{c,a1}$ and $h_{r,a}$ are the heat coefficient of the convection and the radiation process at the back PV module's surface (W/Km^2), respectively. T_{pv}, T_{amb}, T_{sky} and T_{wo} represent the temperature at the back surface of the PV module, the ambient, the sky and the exterior surface of the building wall (^{o}C), respectively. T_a is the temperature of the air mass inside the gap (^{o}C), which is assumed to be an average between the inlet and the outlet air's temperature as given below:

$$T_a = \frac{T_{a,o} + T_{a,i}}{2}, \tag{6}$$

where $T_{a,i}$ is the air temperature at the inlet of the gap, which is assumed equal to T_{amb}, and $T_{a,o}$ is the air temperature at the outlet of the gap (^{o}C).

a. Heat Convection

The heat convection occurs at the front surface of the PV module ($q''_{c,f}$), which is a combination effect between forced convection due to wind speed and natural convection due to the difference in temperatures between that at the PV module surface and the ambient air. The coefficient of the combination effect can be equated by the formulae as proposed by Duffie [7] shown below:

$$h_{c,f} = h_{c,fw} + h_{c,fn}, \tag{7}$$

when

$$h_{c,fw} = 2.537\sqrt{\frac{2(W+L)V_w}{WL}}, \tag{8}$$

$$h_{c,fn} = 9.482\sqrt[3]{\frac{|T_{pv} - T_{amb}|}{7.328 - |\cos\theta|}}, \tag{9}$$

where $h_{c,fw}$ and $h_{c,fn}$ are the heat coefficient of the force convection due to the effect of wind speed and that of the natural convection due to the temperature difference (W/Km^2), respectively. L and W are the length and the width of the PV module (m), respectively. V_w is the natural wind speed (m/s) and θ is the tilted angle of the PV module plane installation (degrees).

At the back surface of the PV module, the height of air gap spacing is one of the important parameters to determine the characteristic of a heat convection process inside the gap. The heat convection process in the gap is dominated by a combination effect of natural convection caused by a temperature gradient within the air gap and the force convection due to wind. Natural convection occurs because of the difference in temperatures between that at the back surface of the PV module and the temperature of the air mass inside the gap. Duffie [7] formulated an equation for determining the heat convection coefficient of the air inside a gap as follows:

$$h_{c,a} = \frac{Nu \cdot k_a}{S} \tag{10}$$

where Nu is the Nusselt number, k_a is the thermal conductivity of air (W/Km^2) and S is the spacing distance of the air gap (m).

Generally, the heat convection coefficient in the gap is characterized by the flow condition of the air inside the gap, which can be determined by a dimensionless group of the Nusselt number (Nu). For a vertical parallel plane installation, the Nusselt number (Nu) can be given by [9]:

$$Nu = 0.61\left(\frac{g\beta'\Delta T S^3}{\nu\zeta}\right)^{0.25}, \tag{11}$$

where g is the gravity acceleration (m/s^2), β' is the volumetric coefficient of expansion, which equals $\frac{1}{T'_a}$. ΔT is the temperature difference between two materials (K). ν and ζ are the kinematics viscosity and the thermal diffusivity (m^2/s), respectively.

Recently, Trinuruk [8] found that the heat convection coefficient as given by the empirical formula in Eq.(10) and (11) can give satisfactory results for PV module temperature prediction only when it was applied for air gap spacing less than 20 mm. If the gap is larger than this critical limit value, the errors of the temperature prediction for the back surface of the PV module and for the exterior surface of the building envelope are increased enormously. Therefore, it was concluded that the heat convection coefficient at the back surface of the PV module in Eq.(10) and (11) were suitable only for spacing less than 20 mm. In order to calculate the heat convection coefficient at the back surface of the PV module for a space greater than 20 mm, Eq.(7) was adopted for the calculation instead. The results of the study confirmed that, for a large air gap the heat convection process inside the gap was quite similar to the heat convection process at the front surface of the PV module. This is because when the height of an air gap is large enough, it is sufficient to allow air flowing freely into the gap, similar to the condition of an open-rack mounting.

b. Long Wave Radiation

Long wave radiation processes occur on two surfaces of the PV module. The first one is at the front surface of the PV module which mainly exchanges with the sky temperature. Its radiative coefficient is given below [9]:

$$h_{r,f} = \sigma\varepsilon_{pv} \cdot \left(T'^2_{pv} + T'^2_{sky}\right) \cdot \left(T'_{pv} + T'_{sky}\right), \quad (12)$$

where σ is the Stefan-Bozlmann constant (W/m^2.K^4), ε_{pv} is the emissivity of the front surface of the PV module. T'_{pv} and T'_{sky} represent the absolute temperature of the PV module and of the sky (K), respectively. The absolute sky temperature can calculated based on the Idso-Jackson model [10] as shown below:

$$T'_{sky} = \sqrt[4]{\frac{R_o + (\sigma T'^4 - R_o)F}{\sigma}}, \quad (13)$$

where R_o is the downward atmospheric radiation flux from a clear sky, T' is the absolute screen level air temperature (K) and F is the correction factor from the effect of clouds [11].

The second long wave radiation exchange process occurs at the back surface of the PV module and the exterior surface of the building envelope. The radiation coefficient can be written as follows [9]:

$$h_{r,a} = \frac{\sigma(T'^2_{pv} + T'^2_{wo})\left(T'_{pv} + T'_{wo}\right)}{(1/\varepsilon_{td}) + (1/\varepsilon_{slab}) - 1}, \quad (14)$$

where T'_{wo} is the absolute temperature of the exterior surface of the building envelope (K), ε_{td} and ε_{slab} are the emissivity of Tedlar, which is the back sheet of the PV module, and of the outermost surface, the concrete slab of the building envelope, respectively.

c. Accumulated Heat in the PV Module

The amount of heat accumulated within the PV module highly depends on the thermal-physical properties of all components constituted in the PV module. The heat accumulated within an aggregated mass can be estimated as below [3]:

$$q''_{st,pv} = \frac{(mC_p)_{pv}(T_{pv,j} - T_{pv,j-1})}{A_{pv}\Delta t}, \quad (15)$$

and $(mC_p)_{pv} = \sum_{i=1}^{n}\left(m_{pv,i} \cdot C_{p,pv,i}\right)$

$$= \sum_{i=1}^{n}\left(\left(A_{pv,i} \cdot \delta_{pv,i} \cdot \rho_{pv,i}\right) \cdot C_{p,pv,i}\right) \quad (16)$$

where $(mC_p)_{pv}$ is the total heat capacity of the PV module (J/K), $m_{pv,i}$ is the mass of the ith layer component of the PV module (kg), A_{pv} is the surface area of the PV module and $A_{pv,i}$ is the surface area of a component at the ith layer (m^2), which is equal to A_{pv}. $\rho_{pv,i}$, $\delta_{pv,i}$ and $C_{p,pv,i}$ are the density(kg/m^3), the thickness (m) and the specific heat of the ith layer component of the PV module (J/kgK), respectively. $T_{pv,j}$ and $T_{pv,j-1}$ are the temperatures of the PV module at jth and (j-1)th time step (^{o}C), respectively. Δt is the interval time (s).

d. Electricity Generation from the PV Module

The amount of electricity generated (E''_{pv}) is influenced by the operating temperature of the PV module and the intensity of solar irradiance, which can be calculated as shown below [12]:

$$E''_{pv} = \dot{I}_t \eta_{stc} \cdot [1 - a(T_{pv} - T_{stc})], \qquad (17)$$

where η_{stc} is the PV module efficiency at the Standard Testing Condition (STC) of the International Electro-technical Commission (IEC) No. 61215 [13], which specifies that the module's performance testing must be conducted at 1,000 W/m^2 of solar irradiance, and the solar spectral irradiance distribution must comply with the IEC 60904-5 standard, while the cell temperature is kept constant at 25^{o}C , i.e. T_{stc} in Eq.(17) a is the temperature coefficient of the PV module (^{o}C^{-1}), which is equal to 0.5% per ^{o}C for a crystalline module [2].

2.2 Energy Balance of the Air Mass within the Gap

Generally, air flowing through the gap absorbs the heat from the surface of the PV module and the building envelope's surface by heat convection. The heat convection coefficient at the back PV module's surface is assumed to be equal to the heat convection coefficient at the exterior surface of the building wall for a large air gap as explained above in Section 2.1 (a). The absorbed heat is then carried out to the surrounding outside the gap by air mass transfer.

$$h_{c,a1}(T_{pv} - T_a) + h_{c,a2}(T_{wo} - T_a) = \dot{M}_a C_{p,a} \frac{T_{a,o} - T_{a,i}}{A_{pv}} \qquad (18)$$

when

$$\dot{M}_a = C_d \rho_a A_{ent} \sqrt{\frac{2gL_c \sin\theta \cdot (T_a - T_{amb})}{(1 + A_{ext}^2) T_{amb}}}, \qquad (19)$$

and $T_{a,o} = 2T_a + T_{amb}$, (20)

where $\dot{M}_a$ is the mass of the air flowing through the gap (kg/s), which is given by [14], $C_{p,a}$ is the specific heat capacity of the air mass flowing into the gap (J/kg.K). $T_{a,o}$ can be derived from Eq.(6) in term of T_a and T_{amb} as given in Eq.(20). C_d is the coefficient of the discharged air mass, which is 0.57 [15], ρ_a is the density of the air in the gap (kg/m^3) A_{ext} and A_{ent} are the outlet cross section area and the inlet cross section area of the air gap (m^2), respectively. L_c is the characteristic length of PV panel (m), which is $L/2$.

In the case of a four sided air gap, the mass of air can move in and out freely from all ends of the gap. For simplification, it is assumed that the mass of the air moving in and out are equal. Therefore, the air-entrance area and air-exit area of the air mass can be equated to:

$$A_{ent} = A_{ext} = S.(W + L) \qquad (21)$$

2.3 Energy Balance at the Outermost Surface of the Wall

From Fig.1, flowing air inside the gap releases the heat to the exterior surface of the building wall by a heat convective process. However, it also receives radiated thermal energy from the back surface of the PV module (if the temperature at the back surface of the PV module is greater than the exterior surface of the wall). The released heat from the air to the building's surface then penetrates into the building by heat conduction (if the interior surface temperature of the building is lower that of the exterior surface). Therefore, we can balance related energy equations as follows:

$$q''_{c,a2} + q''_{r,a} = q''_{k,w1} \qquad (22)$$

where $q''_{c,a2}$ represents the rate of heat convection at the exterior surface of the building wall (W/m^2), $q''_{r,a}$ is the rate of the thermal radiation exchanged between the exterior surface of the building and the back surface of the PV module (W/m²), $q''_{k,w1}$ is the rate of the heat conduction penetrated into the 1st layer of the building wall (W/m²), which is given as below:

$$q''_{k,w1} = \frac{(T_{wo} - T_{w,1j})}{R_{w,1a}}, \quad (23)$$

when $R_{w,ia} = R_{w,ib} = \dfrac{\delta_w}{2n_w k_w}$, (24)

where T_{wo} is the exterior surface temperature of the building envelope (°C), $T_{w,1}$ is the temperature at the middle of the 1st layer of the building wall's material (°C), $R_{w,1a}$ is the heat conduction resistance of a half thickness of the 1st layer of the building's material (mK/W). For any ith layer, with a temperature node at the mid-point of that layer, $R_{w,ia}$ and $R_{w,ib}$ are the heat resistances of the first half and the second half of the thickness of the ith layer of the building wall (mK/W), as given in Eq.(24), respectively. δ_w is the overall thickness of the building wall (m), k_w is the thermal conductivity of the building wall's material (W/m.K) and n_w is the number of total finite layers of the building's wall, designated for thickness calculation.

For a thick building envelope, it is unreasonable to assume that the entire temperature of the wall's thickness are uniform, a dimensionless group of Biot number (Bi) is applied in this case to determine the number of reasonably designated finite layers for the building envelope in order to achieve a series of uniform temperatures for the building envelope's layers. Bi is generally assigned to be less than 0.1, and its equation is given below [16]:

$$Bi = \frac{h_{c,w}\delta_w}{2n_w k_w}, \quad (25)$$

where $h_{c,w}$ is the heat convection coefficient of the exterior surface of the wall (W/m²K).

2.4 Energy Balance in the Wall

The heat transfer across the wall's thickness can be simplified by one-dimensional transient heat conduction analysis. The backward finite difference method is used to analyze the energy balance for any interior point inside the wall as show in Fig.2. Since only a portion of heat is transferred to further inner adjacent layers by heat conduction, the rest is still stored in that layer as shown below:

$$\frac{T_{w(i-1)} - T_{wi}}{R_{(i-1)b} + R_{ia}} - \frac{T_{wi} - T_{w(i+1)}}{R_{ib} + R_{(i+1)a}}$$

$$= \frac{(T_{wi,j} - T_{wi,j-1}) \cdot m_w C_{p,w}}{(t_j - t_{(j-1)}) \cdot n_w}, \quad (26)$$

where $T_{w(i-1)}$, T_{wi} and $T_{w(i+1)}$ are the temperature of the building wall on the layer of the (i-1)th, ith, (i+1)th, respectively (°C). $T_{wi,j}$ and $T_{wi,j-1}$ are the temperature of the building wall on the ith layer at jth hour and at (j-1)th hour, respectively (°C), t_j and $t_{(j-1)}$ are the length of hour at jth hour and at (j-1)th hour, respectively. And m_w is the mass of the building wall (kg).

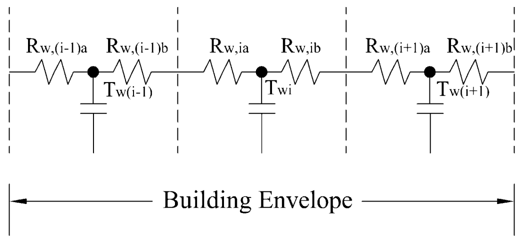

Fig. 2 Thermal network of heat conduction in building envelope material.

2.5 Energy Balance at the Innermost Surface of the Building Wall

The net heat penetration into a room's space of the building is characterized by the temperature at the innermost interior surface of the building, coupled with a room ambient temperature, by the heat convection and the thermal radiation, which becomes a cooling load of the air conditioning system of the building. The heat balance between incoming heat into the innermost layer of the building wall and the outgoing heat released to the indoor air of a room's space can be given by:

$$h_i(T_{wi} - T_i) = \frac{T_{n,j} - T_{wi}}{R_{w,nb}}, \qquad (27)$$

where h_i is the overall heat transfer coefficient of the combination heat transfer process of the thermal convection and radiation at the innermost surface of a room (W/m^2.K), T_{wi} is the temperature at the innermost surface of a room's wall (^{o}C), T_i is the indoor air temperature of the room's space (^{o}C).

American Society of Heating, Refrigerating and Air Conditioning Engineers (ASHRAE) recommends that the overall heat coefficient of the combination heat transfer process of the convection and thermal radiation at the interior wall surface of a room should be 8.3 W/m^2.K for an indoor condition during the summer time in a temperate climate [17], which is somewhat similar to the normal indoor condition of a tropical climate. Thus, the value of 8.3 W/m^2.K was adopted for the overall heat transfer coefficient of the innermost surface of the wall in this study.

3. Criteria for Verification and Simulation in this Study

For simplicity, some conditions of the testing for verification were fixed as follows: (a) The structure of a wall was constructed similar to a common conventional wall in Thailand, which is made of light weight concrete blocks plastered with concrete mortar on both surfaces, as given in Fig.3. The material properties of the PV module and the components of the building wall are given in Table 1. (b) The ratio of the surface areas between the installed PV module's and the building envelope's were overlaid equally at the ratio of 1:1, with no window areas. (c) The indoor ambient temperature of the room was controlled constantly at 25^{o}C as this temperature is a common value for comfortable air conditioning temperature in Thailand. (d) An air gap between the PV module and the outmost exterior surface of the wall was created; four-side-ends of the PV module were fully opened and exposed to the surroundings. Thus, the natural air can flow freely through the gap. (e) The orientation of the PV module is due southward under the clear sky condition of Thailand in March. It should be note that, normally, the maximum solar irradiance is peak during December to January. Unfortunately, due to some difficulties in the field experimental platform setting up, therefore, the experiment was delayed and conducted in the clear sky condition of March instead.

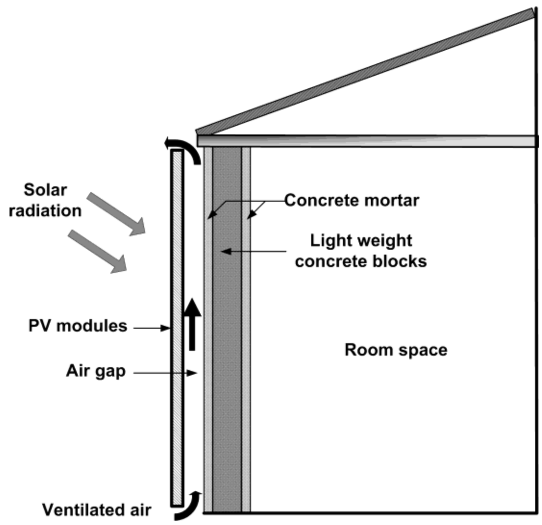

Fig. 3 The installation of PV module over a conventional building envelope of Thailand.

4. Simulation Procedures

Based on the energy model described above, a simulation model was developed by using MATLAB software as a tool for this simulation. The simulation aimed to evaluate the annual amount of electrical energy generated by a PV module and the annual amount of heat gain penetrated into a building, which were calculated by Eq.(17) and Eq.(27), respectively. In order to achieve the results mentioned above, the main unknown parameters for this calculation under this condition were the temperatures at the back surface of the PV module, the outermost exterior and the innermost interior surface temperature of the wall of a building envelope and a temperature of each divided layer across the thickness of the wall.

By solving those unknown temperatures, several data of the climate were necessary for input into the model for a time step of one-hour period. To predict the maximum possible annual amount of electricity generation and the maximum possible annual amount of heat gain penetration into the building, the input climatic condition of the model was assumed to be under clear sky conditions. Revised ASHRAE clear sky model [22], ASHRAE air temperature model [23] and Idso-Jackson model [10-11] were adopted to simulate the climatic data of Bangkok for global solar irradiance, ambient temperature and effective sky temperature, respectively. In this study, the mean day of the month as recommended by Duffie [7] was used as a representative day for each month to determine monthly averaged hourly solar irradiance under clear sky conditions.

In this simulation, the conditions of the PV module's installation was assumed to be similar to that of the verification: i.e. PV module was vertically fixed over the system wall and facing southward, since this is the condition at which the wall receives the maximum amount of solar irradiance falling on the PV module's surface over an entire year. Spacing of the air gap was varied from 0 to 100 mm, with an increment of 5 mm. After the gap had reached 100 mm the gap spacing was then varied with increments of 25 mm until it reached 300 mm.

Since an initial guess of all temperature parameters was required at the beginning steps of the simulation, all unknown temperatures were assumed to be at the same value of 25^{o}C. Moreover, in order to obtain precise results of the temperatures prediction, the acceptable difference between the guessed temperature and the predicted one for each loop of the iteration was limited to be not more than 0.001^{o}C.

5. Verification Procedures

An outdoor testing rig was constructed to replicate an actual PV module installation over a building wall, but with a much smaller size, as illustrated in the schematic diagram of Fig.4. The experiment was carried out under a climate of clear sky conditions in Bangkok, Thailand, in the month of March 2007.

In Fig.4, the testing rig consists of a 80W multi-crystalline silicon PV mounted over and parallel to a light weight concrete building wall separated by an air gap. The light weight concrete wall was enclosed with an insulated box, which was replicated as a room of a building. The ambient temperature of the internal space of the room was controlled to be constant at 25±1^{o}C by an air conditioning unit. The mentioned testing rig was designed in such a way that the air gap spacing between the back surface of the PV module and the outermost surface of the wall can be adjusted to any desired gap space up to 500 mm.

For measuring observations, calibrated K-type thermocouples were attached at the mid point of the front and the back surface of the PV module, of the outermost exterior and the innermost interior surface of the wall. Their positions are shown above as No.1, 2, 4 and 7 in Fig. 4, respectively. Temperature sensors were also installed within the air gap and within the inner space of the insulated box. In addition, a weather station was also installed close to the testing rig. It was equipped with a pyranometer, which was mounted on the same plane as of the PV module's surface vertically, to measure incoming solar irradiance falling on the PV module's surface. A four-blade propeller anemometer with a wind vane was used to measure wind speeds and directions. A temperature probe, made of a shielded thermistor, equipped in the weather station was used for measuring the ambient temperature. The observations were sampled every 10-seconds and then averaged over each one-hour periods. Electrical signals were recorded by data loggers for data collection. Electrical current generated by the PV module was connected to a battery of 12-V with fixed voltage, which served as an external load of the PV module.

Table 1 Physical properties of the PV module's components and building materials [8, 18-21]

	Unit	Glass	PV cell	Tedlar	Lightweight block	Concrete plastered
Thickness	m	0.006	0.00038	0.000037	0.075	0.01
Density, ρ	kg/m^3	2,500	2,330	1,475	700	1,400
Specific heat, C_p	J/kg.K	840	712	1,130	853	1228.7
Thermal conductivity, k	W/m.K	1.04	148	0.14	0.1945	0.5868
Absorptivity, α	-	0.8*	-	-	-	0.4
Emissivity, ε	-	0.94	-	0.893	0.93	0.6

Note: * is the absorptivity-transmittivity of the PV module

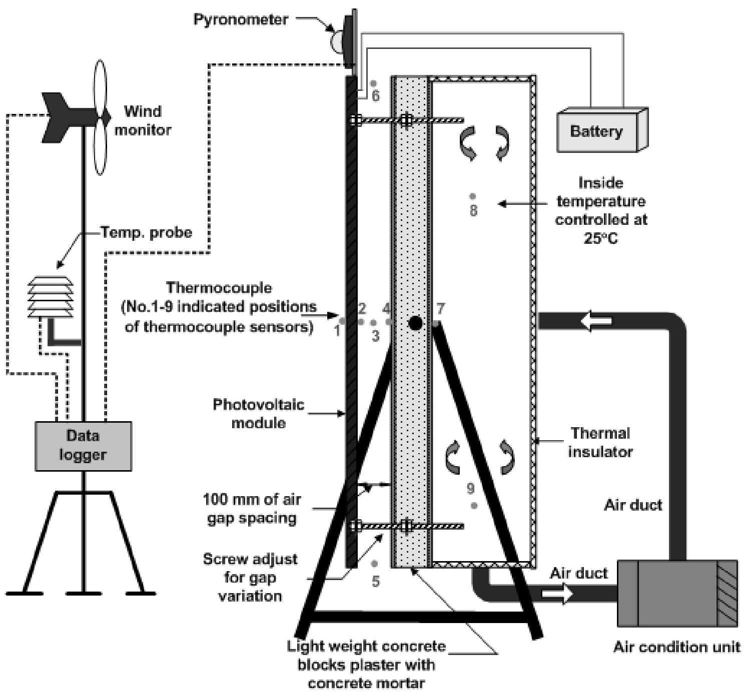

Fig. 4 Schematic of a PV module on a building wall

6. Results and Discussions

6.1 Verification of the Simulation's Results

Before applying the simulation model for evaluating the annual amount of heat flux penetrating into a building wall and the annual electrical energy generated by the PV module under clear sky conditions of Thailand, the simulation model had been verified for its correctness of the temperature prediction for each surface compared to the actual measured data as discussed below.

Fig.5 shows the simulation results of the predicted temperatures of three surfaces: the back surface of the PV module, the outermost exterior surface of the wall and the innermost interior surface of the wall, compared with those of observations. The statistical analysis of those results is summarized in Table 2. It indicates that the simulation results of the developed model were in good agreement with the observed temperatures. The square of the correlation coefficient, R^2 was more than 0.86 except for the innermost wall's surface where R^2 is about 0.82. The Root Mean Square Error (RMSE) was less than 1.40^{o}C for observations of all three surface's temperatures. The corresponding Mean Bias Errors (MBE) was slightly biased with under-estimation, but not greater than 0.70 ^{o}C (in absolute terms).

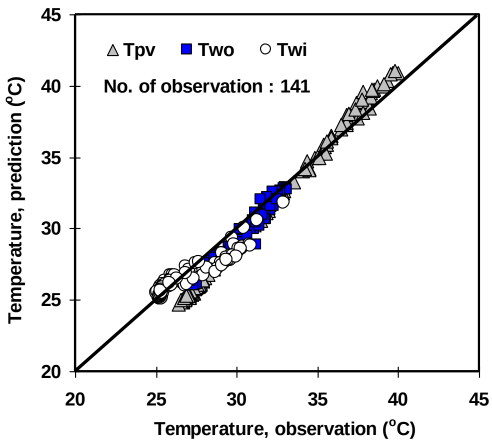

Fig. 5 The correlation between the measured and the predicted surface temperatures of the PV module installation over a building wall in the vertical installation

The lower value of R^2 for the temperature of the innermost wall's surface was caused by the fact that the room's temperature was controlled to be constant at 25^{o}C. Thus, all plotted co-ordinate points of the predicted and the observed temperatures tended to be clustered at a single point of the co-ordinate, at the specific temperature close to 25^{o}C.

Table 2 The statistical analysis of the predicted temperatures by the simulation model

Temperature	R^2	RMSE (^{o}C)	MBE (^{o}C)
The back surface of the PV module	0.919	1.311	-0.685
The exterior surface of the building wall	0.865	0.784	-0.685
The interior surface of the building wall	0.819	0.791	-0.256

6.2 Diurnal Variations of the PV Module's Temperatures and Building Wall's Temperatures

Fig.7 presents the temperature profiles of the observed and the predicted temperatures with respect to the change of solar irradiance within a day. The results show good agreement between the observed and the predicted temperatures. As expected, the peak temperature of the PV module took place when the intensity of solar irradiance was maximum. Meanwhile, the peak temperatures at the outmost exterior and at the innermost interior surface of the wall were delayed later than the peak of solar irradiance for about two and four hours, respectively.

The delay of the peaks at the outermost exterior and the innermost interior surface of the wall, as compared to the peak temperature of the PV module, were due to a difference in the heat capacitance between the mass of the wall and that of the PV module. The properties of materials of the wall and the PV module are given in Table 1. It clearly shows that the building material has higher thermal capacity than that of the PV module. Thus, the wall can absorb and store more heat than the PV module. As a result, the peaks of the wall's surface temperatures were delayed due to the effect of thermal inertia.

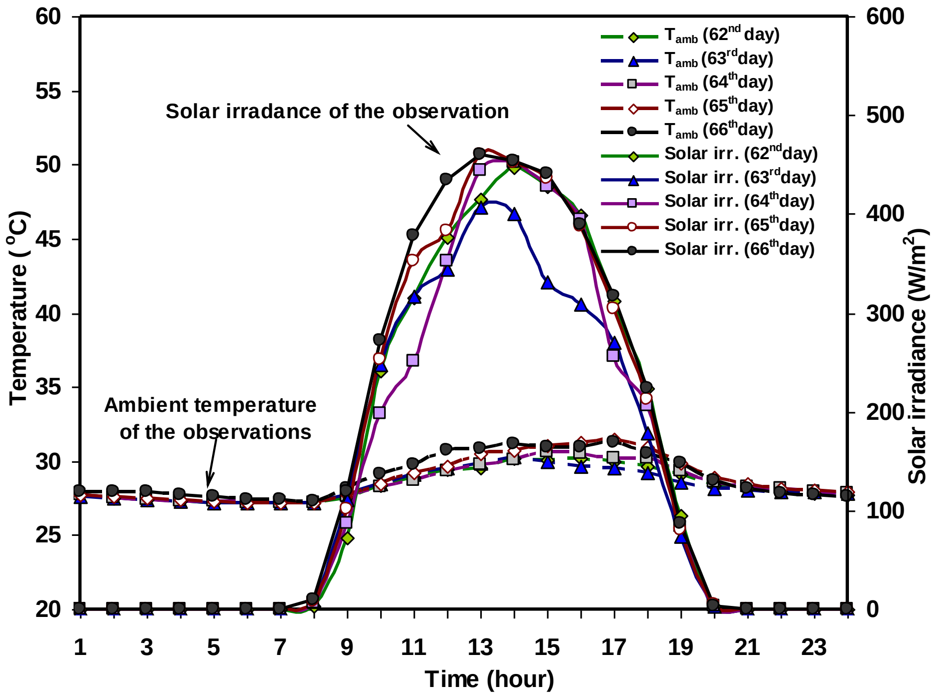

Fig. 6 Ambient conditions of the observations (Numbers in the bracket are Julian day of the year)

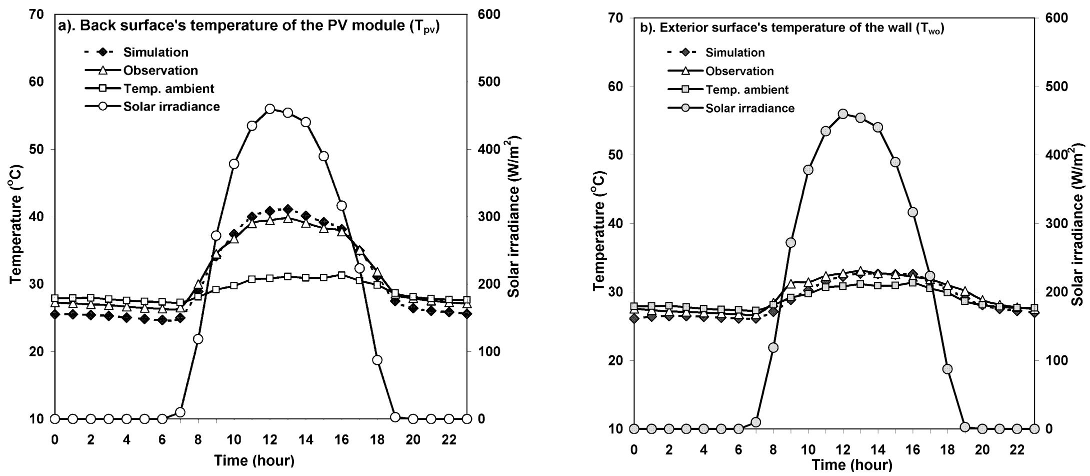

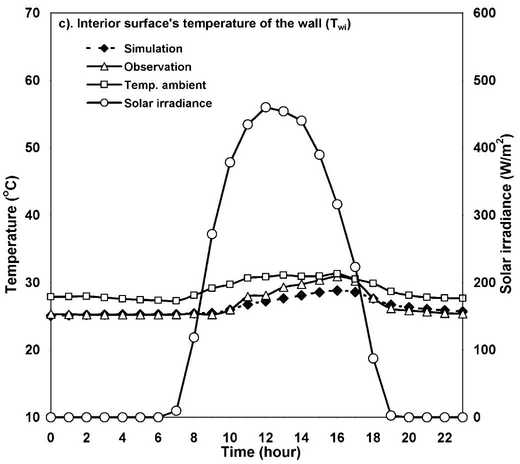

Fig. 7 Hourly temperature profiles of the measured and the predicted temperatures of four-ends (open) of the vertical PV installation with 10 cm air gaps, facing southward.

6.3 Effect of the Air Gap's Height on the Annual Amount of Penetrated Heat Gain into the Building and the Annual Amount of Electrical Energy Generated by the PV Module

Since the predicted results of the developed model were in good agreement with the actual observations, the simulated model was then applied further to simulate the amount of heat gains penetrated into the building and the amount of electrical energy generated by the PV module over an entire year under clear sky conditions of Bangkok, with the assumption that the wind speed is below 1 m/s throughout a year. Only the PV module which was installed vertically and was fixed to a wall due south was taken into consideration in this study. Various air gap spacings were simulated under the conditions mentioned above.

The simulated results of the heat gain and the generated electricity were plotted versus the spacing of the air gap as shown in Fig.8. It is obvious that the relationships between the heat gain and the air gap, and the electricity and the air gap, are not linearly proportional to the air gap's spacing. As shown in Fig.8, the amount of heat penetrated into the building reduced sharply at small gap spacing, and then it gradually decreased as the spacing of the air gap increased. On the other hand, the electricity generated by the PV module increased as the spacing of the air gap enlarged. However, the percentage of changes in the annual amounts of heat gain was much more sensitive than the percentage of changes in the annual amounts of electricity generated when the spacing of the air increased. For example, the heat gain reduced by 6.82%, while the generated electricity increased only 0.27%, when the spacing of air gap increased from 5 mm to 10 mm. So it can be concluded that the change of the air gap has a more strong effect on the reduction of the annual amount of heat gain penetrated into the building than an increase in the benefit of the annual amount of electricity generation from the PV module.

At very small air gap spacing, the penetrated heat gain into the building is considerably high, as compared to a normal air gap spacing, because the cross section area of the air gap's entrance is quite small, to allow the natural air flowing into the air gap. The natural convection due to the difference of the temperatures at the back surface of the PV module and that at the outermost exterior surface of the wall is, therefore, the strongly dominant overall heat transferring process, while the effect of the wind speed from outside is insignificant. However, as the spacing of air gap increased, the cross section area of the air gap entrance is enlarged. Thus, the wind's effect from the outside increases, and the forced convection due to the air flowing into the air gap is more influential. So the amount of heat in the air gap can be transferred more to the surrounding area. This results in decreasing the temperature at the back surface of the PV module, as well as the temperature at the outermost exterior surface of the wall.

As one can see in Fig.8, when the enlargement of the air gap spacing is 50 mm or larger, the rate of change in reduction of the amount of heat gain penetrating into the building is insignificant. The rate of change of the amount of electricity generation by the PV module does not increase significantly.

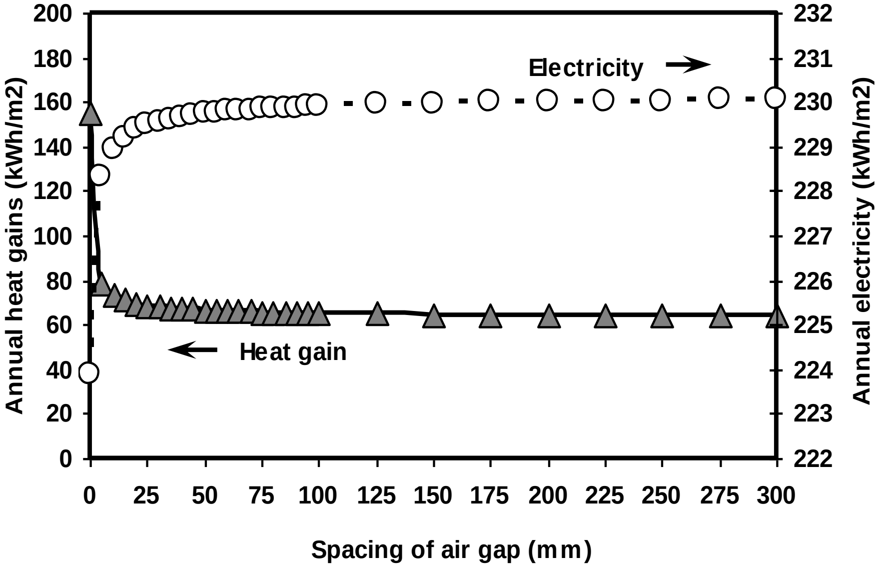

Fig. 8 The simulation results of the annual heat gains and the electricity generation from the PV module for the vertical installation fixed to the wall at various air gap spaces.

Therefore, it can be concluded that the recommended minimum spacing of the air gap should not be less than 50 mm in order to minimize the amount of the heat transferred into the building and to maximize the electricity output. Although an increase of the air gap spacing tends to reduce the heat gain through the building, at the same time, it also increases the electricity generation. However, in practice, the spacing of the air gap is limited to a certain point. This is because when the gap is too large, direct sunlight can easily pass through the gap and results in more unprotected non-shaded area (by the PV module) on the outermost exterior surface of the building. This will result in a rise of temperatures at the exterior surface of the building's wall due to the direct solar irradiance. This can cause more heat gain penetrating into the building. For a small air gap, the non-shaded area is small and its effect is insignificant.

6.4 Comparison of Heat Gain Penetration through a Building Facade: One with and One without an Installation of a PV Module as a Shading Device

According to the criteria of the simulation's conditions in Section 3, the results of the simulation for the heat gain penetrating through the facade of a building between one with and one without an installed PV module were also compared in this research. It was found that an installation of the PV module onto the exterior surface of a convectional building envelope with a proper air gap space can reduce the cooling load of the building about 116,000 kJ/m^2 per year, as given in Fig.9. The reduction of the cooling load is due to the shading effect of the mounted PV module, which can prevent the heat load due to the solar irradiance falling on the building's surface. The presence of a ventilated air gap also helps to carry out a little heat behind the PV module to the surrounding area.

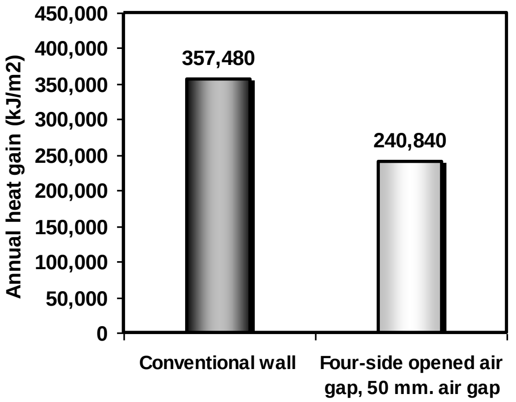

Fig. 9 Comparison of the annual heat gains penetrated into the conventional building wall, with and without a PV module installation.

In addition, it was noticed that the absorptivity of the material property plays an important role in the thermal capability in absorbing heat radiation. High absorptivity results in high heat absorbtion within the material. Consequently, it can intensively absorb a large amount of heat, which in turn penetrates further into the building. In this study, the absorption of the PV module (0.8) is twice that of the building wall's (0.4). As a result, the PV module absorbs a large amount of heat from the solar irradiance, which in turn will radiate thermal heat to the building's surface. Eventually, this transferring could cause a large heat gain into the building envelope if the air gap is not properly designed.

7. Conclusions

The investigated results in this study indicate that the developed simulation model based on one dimensional transient heat transfer with four-opening ends (air gap) of an installed PV module over a building envelope gives good satisfactory results in prediction with R^2 = 0.86 for all surface temperatures, except the one at the innermost interior surface of the building wall, in which R^2 is 0.82, and the largest value of RMSE is less than ±1.40°C.

The installed PV module on a conventional building envelope plays an important role, not only generating clean electricity, but also reducing heat gain penetrating into the building, provided that the air gap must be properly designed to cool down the temperature of the PV module. Moreover, the amount of heat penetrated into the building can be reduced when the PV module is installed as a shading device to prevent the exterior surface of the building envelope from short wave radiation of the sun. Air gap ventilation is necessary when a PV module is installed in tropical climates like Thailand. It helps natural air to carry away heat from the PV module. A minimum space of 50 mm for the gap is recommended for the vertical PV module installation with southward facing walls in the tropics.

Although spacing of an air gap for a PV module installation plays an important role in reduction of heat gains penetrating into a building, it does not help to improve amounts of electricity generation by the PV module. Therefore, the designation of an appropriate air gap space should be judged on the amounts of the heat gain reduction into the building rather than on the electrical generation performance of the installed photovoltaic system.

8. Acknowledgements

P.Trinuruk would like to express her gratitude to the Joint Graduate School of Energy and Environment (JGSEE), Energy Policy and Planning Office (EPPO), Ministry of Energy and Center for Energy Technology and Environment (CEE), S&T Postgraduate Education and Research

Development Office (PERDO), Ministry of Education of Thailand for supporting the study at JGSEE and for the research funding. The authors would like to give special thanks to Dr. Dhirayut Chenvidhya, the Director of Clean Energy System Group (CES) for his valuable advice. Appreciation is also given to staff of Clean Energy System Group (CES), King Mongkut's University of Technology Thonburi, for their assistance to set up an experiment platform.

9. References

[1] Mingvimol, U. and Boonyatikarn, S., An Approach to Formulate Energy Conservation Evaluation Index in Residential Buildings, Chulalongkorn University, Thailand, 1997.

[2] The German Solar Energy Society and Ecofys, Planning and Installing Photovoltaic System: A Guide for Installers, Architects, and Engineers, James & James (Science Publishers) Ltd., England, 2005.

[3] Brinkworth, B.J., Cross, B.M. Marshall, R.H. and Yang, H.X., Thermal Regulation of Photovoltaic Cladding, Solar Energy, Vol.61, No.3, pp.169-178, 1997.

[4] Yang, H.X., Marshall, R.H. and Brinkworth, B.J., Validated Simulation for Thermal Regulation of Photovoltaic Wall Structures, 25th PVSC, May 13-17, Washington, D.C., pp. 1453-1456, 1996.

[5] Krauter, S., Araujo, R.G., Schroer, S., Hanitsch, R., Salhi, M.J., Triebel, C. and Lemoine, R., Combined Photo-voltaic and Solar Thermal Systems for Facade Integration and Building Insulation, Solar Energy, Vol. 67, No.4-6, pp. 239-248, 1999.

[6] Wang Y, Tian W, Ren J, Zhu L, Wang Q. Influence of a Building's Integrated-Photovoltaics on Heating and Cooling Loads, Applied Energy, Vol.83, pp.989-1003, 2006.

[7] Duffie J.A., Beckman W.A, Solar Engineering of Thermal Processes, New York, Willey, 1991.

[8] Trinuruk P., Sorapipatana C. and Janwitthaya, D., Electricity Generation and Heat Gain on Photovoltaic Roofs in Thailand, Academic thesis of The Joint Graduated School of Energy and Environmental, King Mongkut's University of Technology Thonburi, Thailand, 2006.

[9] Pratt AW. Heat Transmission in Buildings, John Wiley & Sons, Inc., Northern Ireland, 1981.

[10] Idso, S. B. and Jackson, R.D., Thermal Radiation from the Atmosphere. J. Geophys. Res., Vol.74, pp. 5397-5403, 1969.

[11] Exell, R.H.B., Atmospheric Radiation in a Tropical Climate, AIT Research Report, Vol.71, 1978.

[12] Sandnes, B. and Rekstad, J., A Photo-voltaic/ Thermal (PV/T) Collector with a Polymer Absorber Plate, Experi-mental Study and Analytical Model, *Solar Energy*, Vol. 72, (1), pp.63-73, 2002.

[13] International Standard IEC 61215: Crystalline Silicon Terrestrial Photo-voltaic (PV) Modules-Design Quali-fication and Type Approval; 2005.

[14] Mathur, J., Mathur, S., and Anupma, Summer-Performance of Inclined Roof Solar Chimney for Natural Ventilation, Energy and Building, Vol. 38, pp.1156-1163, 2006.

[15] Anderson, K.T., Theoretical Consi-deration on Natural Ventilation by Thermal Buoyancy, Trans. ASHRAE, Vol.101, No.2, pp. 1103-1117, 1995.

[16] Nijaguna, B.T., Thermal Science Data Book, Tata McGraw-Hill, India, 2005.

[17] ASHRAE, Handbook of Fundamen-tals, ASHRAE, Atlanta, USA, 2001.

[18] Cengel, Y.A. and Boles, M.A., Thermodynamic: An Engineering Approach, 2nd Ed., McGraw-Hill Inc.,

USA, 1994.

[19] Davis, M.W., Dougherty, B.P., and Fanney, A.H., Measured Versus Predicted Performance of Building Integrated Photovoltaic, J. Solar Energy Engineering by ASME, Vol. 125, February, pp.21-27, 2003.

[20] Jones, A.D. and Underwood, C.P., A Thermal Model for Photovoltaic Systems, Solar Energy, Vol.70, No.4, pp. 349-359, 2001.

[21] Davis, M.W., Dougherty, B.P. and Fanney, A.H., Prediction of Building Integrated Photovoltaic Cell Temperatures, Trans. ASME J. Heat Transfer, Vol.123, August, pp.200-210, 2001.

[22] Amarananwatana, P. and Sorapipatana, C., An Assessment of the ASHRAE Clear Sky Model for Irradiance Prediction in Thailand, The Joint Graduated School of Energy and Environmental, King Mongkut's University of Technology Thonburi, Thailand, 2005.

[23] ASHRAE, 1993 ASHRAE Handbook-Fundamental, Atlanta, American Society of Heating, Refrigerating and Air Conditioning Engineering, Inc., 1993.